A Method for Reconstruction of Temperature Height Profiles above Active Regions on the Sun by Multifrequency Radio Observations

T. I. Kaltman[1] and A. G. Stupishin[2]

[1] Special Astrophysical Observatory, Russian Academy of Sciences, Nizhny Arkhyz, Russia,
arles@mail.ru
[2] Saint Petersburg State University, Saint Petersburg, Russia

Abstract. A method for reconstructing of height temperature profiles over solar active regions in the upper part of the transition region and in the lower corona from multi-frequency radio observations is presented. The method is based on modeling of radio emission in a magnetic field reconstructed from photospheric measurements. Stratified gyroresonance radiation is calculated together with a continuum bremsstrahlung. The system of equations for iterative search for temperature values at different altitudes includes regularizing equations that relate temperatures at neighboring altitudes. The possibility of reconstructing several temperature profiles over different zones of active region has been developed. The method shows high quality of atmospheric parameters recovery on realistic models and is applied to the results of 1D observations on RATAN-600. The method is also applicable to 2D image observations, respectively, with the possibility of more detailed diagnostics. Modeling of radio observations of solar active regions with additional heating sources is promising for diagnostics of temperature profiles of flare-active regions, regions with plasma jets and is widely applicable for reconstruction of atmospheric parameters of various energy-releasing processes.

Keywords: Sun: activity; Sun: transition region; Sun: radio radiation
DOI:10.26119/978-5-6045062-0-2_2020_409

1 Introduction

Decipherment of the information carried by the microwave emission of active regions allows us to study the region with the highest temperature gradients in the solar corona. In Stupishin et al. (2018) a method for reconstructing the high-altitude temperature profile was proposed. The main drawback was that we link the radiation at a certain frequency to a single "effective" height; in fact, emission at the certain frequency generates in the large range of heights. It is also important that both harmonics contribute to the radiation. In addition, the resulting temperature profile could be strongly non-monotonous, which forced the introduction of a special procedure that ensures monotonous temperature growth with height. All this prompted us to look for new approaches to the implementation of the method.

2 Description of the New Method

The main input conditions are the same as in Stupishin et al. (2018): NLFFF-reconstructed magnetic field (Wiegelmann 2004; Fleishman et al. 2017), the same (more precisely, "spherical-layered", but actually flat-layered, since we work in the "flat photosphere" approximation) atmosphere, NT = const. Let's divide the entire height range into a certain set of "working intervals". Each interval will be characterized by a certain amount of height (for example, the center of the interval) h_i and, accordingly, the characteristic temperature T_i.

Let's set a certain altitude profile of the temperature dependence. For each observation frequency $f^{(j)}$ and for each polarization p, we take a modeled radio map, multiplied by a antenna beam (positioned at a selected point in the scan), and consider the contribution $F_i^{(j,p)}$ of each height interval h_i to the total calculated flux $F_{calc}^{(j,p)}$: for each height interval we consider corresponding sum of fluxes for radio map pixels in which the optical thickness (along the LOS upon this pixel) $\tau = 1$ is at the height within the considered height range. Obviously,the optically thin part of the total flow $F_{thin}^{(j,p)} = F_{calc}^{(j,p)} - \sum F_i^{(j,p)}$ remains unaccounted for.

If we take the altitude profile of the atmosphere that differs from the real one, then the model flux $F_{obs}^{(j,p)}$ will differ from the one observed on RATAN-600 at the selected scan point. We can introduce a temperature correction factor α_i for each height interval: $\widetilde{T_i} = \alpha_i T_i$, where $\widetilde{T_i}$ is the corrected temperature (which will be used in the next iteration step). In our thermodynamic equilibrium conditions $F \sim T$ at $\tau = 1$, the corresponding adjusted fluxes $\widetilde{F_i^{(j,p)}} = \alpha_i F_i^{(j,p)}$, and

$$\sum \alpha_i F_i^{(j,p)} = F_{obs}^{(j,p)} - F_{thin}^{(j,p)}. \tag{1}$$

This is a system of linear equations. If there are enough number of observation frequencies, the system is overdeterminated and a solution can be found in the sense of mean least squares. Since it is an ill-posed inverse problem, to regularize the solution we can require that the temperatures at neighboring height intervals should not be differ significantly. To do this, we add the equations $\alpha_i T_i - \alpha_{i+1} T_{i+1} = 0$, taken with some weight accounting in mean least squares solution. After finding new temperatures, we repeat the entire procedure until a stable result is achieved.

Fig. 1 shows the result of the method on a source with a dipole magnetic field and a simple temperature model. The figure shows very good coincidence of model and reconstructed scans and temperature profiles.

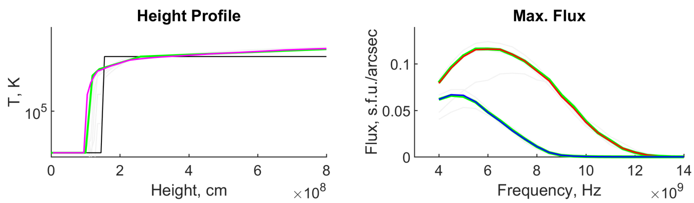

Fig. 1. The temperature profiles (left): model (green), initial (black) and modeled (pink). Coincidence of the calculated and observed spectra (right): model (both R and L green), right (red) and left (blue) polarizations.

3 Discussion and Conclusions

Modeling of radio observations of solar active regions with additional heating sources is promising for diagnostics of temperature profiles of flare-active regions, regions with plasma jets and is widely applicable for reconstruction of atmospheric parameters of various energy-releasing processes. We simulated scans and spectra for a model spot source with dipole magnetic fields and a simple two-step temperature profile, taking into account the convolution with the RATAN-600 beam (Fig. 2). Adding to the temperature profile of a heated section in a narrow layer above the transition zone within the boundaries of the spot quarter segment changes the spectrum, which is also shown on the figure by dashed lines. The difference between the spectra with and without heating can be expressed more or less clearly, depending on the magnitude of the temperature gradient, the area of the hot layer, and the proximity of its location to large values of the magnetic field. The proposed method of temperature profiles reconstruction can be used to detect such hot layers based on radio observations.

As shown by preliminary simulations, the method can be expanded to using observations at several scan points and at different azimuths of the RATAN-600 observations. A promising direction for further development of the method is taking into account that the atmosphere is different over different parts of active

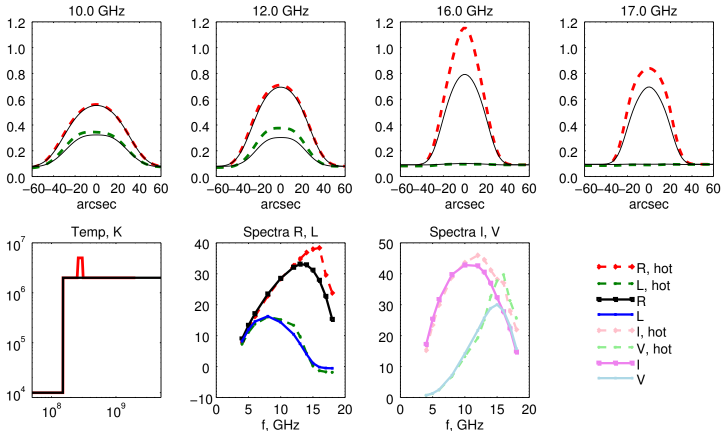

Fig. 2. R and L simulated scans and spectra for the dipole model (solid) and with additional heating (dashed). Bottom left: the model temperature profile (black, additional heating marked by red).

region (umbra, penumbra etc., see, for example, the works of Fontenla [Fontenla et al. (2009)] and many others). Additional information about the temperature and emission measure can be obtained from the UV range, and used for modeling in conjunction with radio emission [Alissandrakis et al. (2019)]. The method is also applicable to 2D image observations, respectively, with the possibility of more detailed diagnostics.

Acknowledgements. The work was supported by RFBR grants 18-29-21016 and 18-32-20165.

Bibliography

Alissandrakis, . E., Bogod, V. M., Kaltman, T. I., Patsourakos, S., & Peterova, N. G. 2019, Sol. Phys., 294, 23

Fleishman, G. D., Anfinogentov, S., Loukitcheva, M., Mysh'yakov, I., & Stupishin, A. 2017, Astrophys. J., 839, 30

Fontenla, J. M., Curdt, W., Haberreiter, M., Harder, J., & Tian, H. 2009, Astrophys. J., 707, 482

Stupishin, A. G., Kaltman, T. I., Bogod, V. M., & Yasnov, L. V. 2018, Sol. Phys., 293, 13

Wiegelmann, T. 2004, Sol. Phys., 219, 87